

Novel triphenylamine-modified ruthenium(II) terpyridine complexes for nickel oxide-based cathodic dye-sensitized solar cells†

Cite this: *RSC Adv.*, 2014, 4, 5782

Christopher J. Wood,^a Kiyoshi C. D. Robson,^b Paul I. P. Elliott,^c Curtis P. Berlinguette^{‡b} and Elizabeth A. Gibson^{*a}

Received 27th August 2013
Accepted 10th December 2013

DOI: 10.1039/c3ra44690e

www.rsc.org/advances

A pair of ruthenium based donor- π -chromophore sensitizers (K1 and K2) have been synthesized for use in NiO based p-type dye sensitized solar cells (p-DSCs). The optical and electrochemical properties of these dyes were determined experimentally and interpreted by DFT modelling. NiO p-DSC devices incorporating these dyes gave photocurrents of 2.9 for K1 and 2.0 mA cm⁻² for K2 (IPCE of 14% and 9%); this is a vast improvement on the photocurrents of p-DSC devices incorporating 'traditional' ruthenium sensitizers.

Introduction

The dye-sensitized solar cell (DSC) is a low cost alternative to crystalline silicon photovoltaic devices that converts sunlight into electricity using a dye adsorbed on a transparent, nano-structured semiconductor electrode, surrounded by a redox electrolyte.¹⁻⁴ Almost all the current research in photocatalysis and dye-sensitized solar cells is focused on n-type semiconductors typically based on TiO₂. Unlike the standard DSC, which has a passive counter electrode, tandem devices use two photoelectrodes, simultaneously, to harvest more light more efficiently.⁵ Incorporation of a photocathode in tandem with a TiO₂-based n-type photoanode in a single device should give rise to a substantial increase in voltage and efficiency.⁶⁻⁸ By choosing sensitizers which absorb the high energy photons on one electrode and low energy photons on the other, more of the solar spectrum can be harvested. Yet tandem DSCs have not yet beaten the best n-type DSCs because the poor performance of dye-sensitized photocathodes limits the overall efficiency.⁹

One of the limitations to NiO-based photocathodes is the fast recombination between the photoreduced dye and holes in the NiO. Previously, it has been shown that significant

improvements to NiO-based p-DSCs can be made by designing organic dyes which promote charge separation and limit the recombination between the sensitizer and/or electrolyte and the semiconductor.^{8,10} Currents obtained in these devices have reached over 5.5 mA cm⁻² at 1 sun illumination but this is considerably less than that achieved with n-DSCs. Typically, when organic photosensitizers are used, the charge-separated state is short-lived ($\tau \approx 20-200$ ps) compared to the regeneration reaction, which must compete in order to collect the charges and produce a photocurrent.¹⁰⁻¹³ Organic dyes perform much better in p-DSCs than ruthenium-based sensitizers.¹⁴ This is possibly a result of the film thickness of NiO films typically used (*ca.* 1-3 μm) being much less than that typically used for TiO₂ in n-DSCs (*ca.* 10 μm) so dyes with higher extinction coefficients maximise the light harvesting efficiency. In addition the optimum geometry for the anchoring group for NiO sensitizers may not have been found. Many organic dyes use one or two benzoic acid groups to couple the dye to the NiO.^{7,15,16} Although ruthenium bipyridyl complexes with various anchoring motifs have been applied, the essential requirements of good charge injection and stability have not been met.^{17,18} We postulated that, if a more stable and conjugated anchoring motif was chosen, we could develop a better ruthenium sensitizer that would make use of the favourable optoelectronic properties of ruthenium sensitizers, in particular the long-lived charge separated state.

Others have since tried to develop ruthenium-based sensitizers using a similar strategy of increasing the spatial separation between the electron acceptor region of the dye and the anchoring group/NiO surface to substantially increase the charge-separated state lifetime.^{19,20} However, whilst incorporating charge-transfer character in the dye design appears to improve the charge-separated state lifetime, the photocurrents generated have still remained low (below 1 mA cm⁻² in ref. 19

^aSchool of Chemistry, The University of Nottingham, University Park, Nottingham, NG7 2RD, UK. E-mail: elizabeth.gibson@nottingham.ac.uk

^bDepartment of Chemistry, University of Calgary, 2500 University Drive Northwest, Calgary, Alberta, T2N 1N4, Canada

^cDepartment of Chemistry, University of Huddersfield, Queensgate, Huddersfield, HD1 3DH, UK

† Electronic supplementary information (ESI) available: NMR spectra for K1 and K2; FTIR spectra of K1 and K2 adsorbed on NiO; emission decay for K1 in methanol; DFT calculations for K1 and K2 in methanol; J-V and IPCE data for K1 with Co(dtb)₃ClO₃(2) electrolyte. See DOI: 10.1039/c3ra44690e

‡ Current address: Department of Chemistry, University of British Columbia, Vancouver, V6T 1Z1, BC, Canada.

and below 2 mA cm^{-2} in ref. 20). Previous success with ruthenium-based push-pull photosensitizers for TiO_2 prompted us to modify our dye-design to suit photocathode sensitization.^{21,22} Here, we report the first of our photosensitizers which are equipped with stable, bidentate anchoring groups, an electron donating amine-thiophene linker with bis-terpyridyl (**K1**) and cyclometalated (**K2**) ruthenium chromophores, depicted in Fig. 1.

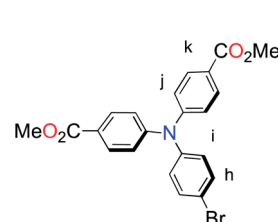
Experimental section

Preparation of compounds

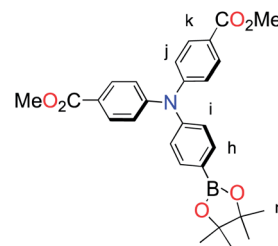
All reactions and manipulations were performed using solvents passed through an MBraun solvent purification system prior to use. All reagents were purchased from Aldrich. Purification by column chromatography was carried out using silica (Silicycle: Ultrapure Flash Silica). Analytical thin-layer chromatography (TLC) was performed on aluminum-backed sheets pre-coated with silica 60 F254 adsorbent (0.25 mm thick; Merck, Germany) and visualized under UV light. Routine ^1H and ^{13}C NMR spectra were recorded at 400 MHz and 100 MHz, respectively, on a Bruker AV 400 instrument at ambient temperature. Chemical shifts (δ) are reported in parts per million (ppm) from low- to high-field and referenced to residual non-deuterated solvent. Standard abbreviations indicating multiplicity are used as follows: s = singlet; d = doublet; t = triplet; m = multiplet. The compounds of 4,4'-(4-bromophenylazanediyl)dibenzaldehyde,^{23,24} 4,4'-(4-(4,4,5,5-tetramethyl-1,3,2-dioxaborolan-2-yl)phenylazanediyl)dibenzoic acid,^{23,24} 4'-(5-bromo-2-thienyl)-2,2':6',2'-terpyridine (**P1c**),^{25,26} 4'-chloro-2,2':6',2'-terpyridine (**L2**),²⁷ 4-(5-bromothiophen-2-yl)-6-(3-(trifluoromethyl)phenyl)-2,2'-bipyridine (**P2a**),²⁸ $\text{Ru}(\text{L2})\text{Cl}_3$ (ref. 29) were synthesized as previously reported.

Dimethyl 4,4'-(4-bromophenylazanediyl)dibenzoate (P1a). To a solution of 4,4'-(4-bromophenylazanediyl)dibenzaldehyde^{23,24} (1.00 g, 2.63 mmol) in an acetone-water (50 mL, 4 : 1, v/v), KMnO_4 (2.08 g, 13.2 mmol) was added portion wise at 60°C . The reaction brought to refluxing temperature for 5 h.

The solvent was removed *in vacuo* and basic water (2.0 M KOH, 50 mL) was added. The suspension was filtered through celite to remove the black precipitate. The filtrate was acidified with conc. HCl to give a white precipitate that was filtered and washed with water and dried under an air stream. The solid was dried further by azeotrope with toluene. The white solid was dissolved in MeOH (100 mL) and conc. HCl (1 mL) was added. The mixture was refluxed overnight. After cooling to room temperature, the solvent was removed *in vacuo*. The product was purified by recrystallization from hot MeOH to yield 0.977 g (84.4%) of the product as a white solid. ^1H NMR (400 MHz, CDCl_3): $\delta = 7.90$ (d, 4H, $^3J = 8.9 \text{ Hz } H_k$), 7.42 (d, 2H, $^3J = 8.8 \text{ Hz, } H_h$), 7.05 (d, 4H, $^3J = 8.8 \text{ Hz, } H_i$), 7.00 (d, 2H, $^3J = 8.8 \text{ Hz, } H_i$), 3.88 (s, 6H, H_j); ^{13}C NMR (100 MHz, CDCl_3): $\delta = 166.7, 150.8, 145.5, 133.2, 131.4, 127.9, 124.9, 122.9, 118.4, 55.2$; HRMS (ESI): $m/z = 440.0484$ $[(\text{M} + \text{H})^+]$ (calcd for $\text{C}_{22}\text{H}_{19}\text{BrNO}_4^+$; $m/z = 440.0492$).



Dimethyl 4,4'-(4-(4,4,5,5-tetramethyl-1,3,2-dioxaborolan-2-yl)phenylazanediyl)dibenzoate (P1b). A Schlenk flask under N_2 was loaded with $\text{Pd}(\text{dppf})\text{Cl}_2$ (21 mg, 0.030 mmol), KOAc (0.167 g, 1.70 mmol) and bis(pinacolato)diboron (0.151 g, 0.602 mmol). DMSO (10 mL), stored over molecular sieves and degassed with N_2) and **P1a** (0.250 g, 0.570 mmol) were added to the flask. The mixture was stirred at 80°C for 6 h under N_2 . EtOAc (50 mL) was added to the flask. The mixture was washed with water ($3 \times 50 \text{ mL}$) to remove the DMSO. The organic layer was dried over MgSO_4 , filtered and the solvent removed *in vacuo*. The residue was dissolved in a minimal amount of CH_2Cl_2 and filtered through SiO_2 . The solvent was removed *in vacuo* and the residue recrystallized from MeOH to yield 0.221 g (79.9%) of the product as a yellow solid. ^1H NMR (400 MHz, CDCl_3): $\delta = 7.90$ (d, 4H, $^3J = 8.8 \text{ Hz } H_k$), 7.74 (d, 2H, $^3J = 8.5 \text{ Hz, } H_h$), 7.10–7.06 (m, 6H, H_i, H_j), 3.86 (s, 6H, H_j), 1.33 (s, 12H, H_r); ^{13}C NMR (100 MHz, CDCl_3): $\delta = 166.8, 151.1, 149.0, 136.6, 131.3, 125.1, 124.9, 123.3, 122.9, 84.1, 52.2, 25.1$; HRMS (ESI): $m/z = 488.2249$ $[(\text{M} + \text{H})^+]$ (calcd for $\text{C}_{28}\text{H}_{31}\text{BNO}_6^+$; $m/z = 488.2245$).



Dimethyl 4,4'-(4-(5-(6-phenyl-2,2'-bipyridin-4-yl)thiophen-2-yl)phenylazanediyl)dibenzoate (L1). A THF- H_2O (9 : 1, v/v; 50 mL)

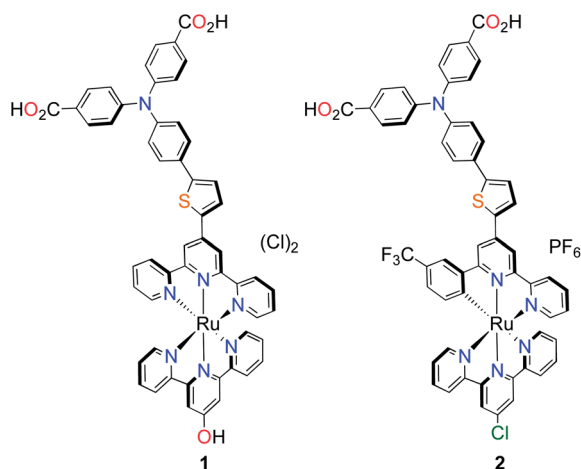
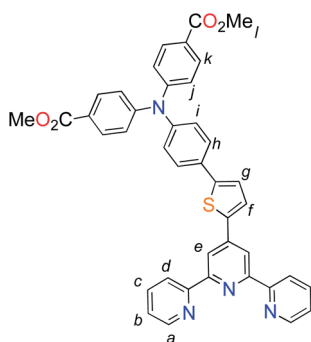


Fig. 1 Molecular structures of p-type polypyridyl (**K1**) and cyclometalated (**K2**) bichromic sensitizers.

solution containing **P1c** (0.327 g, 0.83 mmol), **P1b** (0.570 g, 1.00 mmol), K_2CO_3 (0.881 g, 8.31 mmol) and $Pd(PPh_3)_4$ (96 mg, 0.08 mmol) was refluxed for 20 h under N_2 . The mixture was cooled to room temperature and the solvent removed *in vacuo*. The residue was purified by column chromatography [SiO_2 : CH_2Cl_2 -EtOH, 9.5 : 0.5 v/v R_f = 0.31] to yield 0.196 g (74.3%) of the product as a yellow oil that solidified upon standing. 1H NMR (400 MHz, $CDCl_3$): δ = 8.74 (ddd, 2H, 3J = 4.7, 4J = 2.5, 5J = 0.8 Hz, H_a), 8.69 (s, 2H, H_e), 8.64 (d, 2H, 3J = 7.9 Hz, H_d), 7.93 (d, 4H, 3J = 6.9 Hz, H_k), 7.86 (ddd, 2H, 3J = 7.7, 7.7, 4J = 1.7 Hz, H_c), 7.75 (d, 1H, 3J = 3.8 Hz, H_f), 7.63 (d, 2H, 3J = 8.7 Hz, H_h), 7.37–7.34 (m, 3H, H_b , H_g), 7.16–7.12 (m, 6H, H_i , H_j), 3.89 (s, 6H, H_l); ^{13}C NMR (100 MHz, $CDCl_3$): δ = 166.8, 157.6, 156.7, 156.3, 150.9, 149.3, 146.0, 145.2, 143.2, 141.1, 139.5, 131.3, 130.8, 129.0, 126.5, 124.1, 122.9, 121.7, 116.5, 113.5, 55.20; HRMS (ESI): m/z = 675.2054 [$(M + H)^+$] (calcd for $C_{41}H_{31}N_4O_4S^+$: m/z = 675.2061).

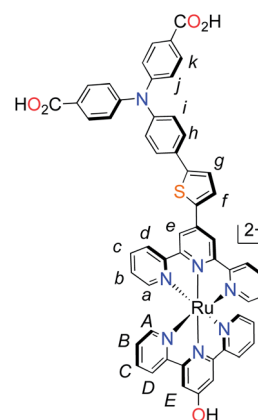


Ru(L1)Cl₃ (1a). In a 250 mL round-bottom flask **L1** (0.110 g, 0.160 mmol) was dissolved in abs. EtOH (150 mL) to give a fluorescent yellow solution. $RuCl_3 \cdot 3H_2O$ (0.055 g, 0.210 mmol) was added and the solution was refluxed for 4 h. The volume of the solution was reduced (~25 mL) and the solution put in the freezer to cool. The brown precipitate was filtered, washed with abs. EtOH, and Et_2O and left to dry to give 0.136 g (94.6%) of the product as a brown solid. HRMS (MALDI-TOF): m/z = 846.0403 [$(M - Cl^-)^+$] (calcd for $C_{41}H_{30}Cl_3N_4O_4S$ = 846.0403); Anal. calcd for $C_{41}H_{30}Cl_3N_4O_4RuS$: C, 56.39; H, 3.49; N, 6.26. Found: C, 56.15; H, 3.68; N, 6.11%.

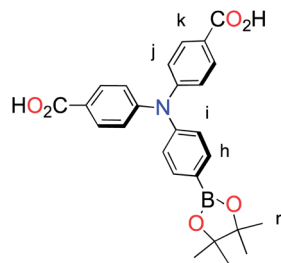
[Ru(L1)(L2)][(NO₃)₂] (1b). In a 250 mL round-bottom flask, **1a** (0.130 g, 0.150 mmol) and **L2** (39 mg, 0.15 mmol) was dissolved in 95% EtOH (150 mL) with *n*-ethylmorpholine (0.1 mL). The solution was refluxed for 18 h. $AgNO_3$ (75 mg, 0.44 mmol) was added and the solution reflux for an additional 2 h. The solvent was removed *in vacuo* and the product purified by column chromatography [SiO_2 : acetone-MeOH- $KNO_3(aq)$ (6 : 1 : 1, v/v/v), R_f = 0.66] to yield 99 mg (58%) of the product as a red solid. 1H NMR (400 MHz, $CDCl_3$): δ = 9.21 (s, 2H, H_E), 8.99 (s, 2H, H_e), 8.88 (d, 2H, 3J = 8.1 Hz, H_D), 8.63 (d, 2H, 3J = 8.1 Hz, H_d), 8.50 (d, 1H, 3J = 4.0 Hz, H_f), 7.98–7.93 (m, 8H, H_C , H_k , H_c), 7.83 (d, 2H, 3J = 8.6 Hz, H_h), 7.69 (d, 1H, 3J = 3.8 Hz, H_g), 7.49 (d, 2H, 3J = 4.7 Hz, H_A), 7.38 (d, 2H, 3J = 4.7 Hz, H_B), 7.28 (d, 2H, 3J = 8.6 Hz, H_i), 7.22–7.16 (m, 8H, H_j , H_a , H_b), 3.87 (s, 6H, H_l); HRMS (MALDI-TOF): m/z = 1043.1584 [$(M)^+$] (calcd for $C_{56}H_{40}ClN_7O_4RuS^+$: m/z = 1043.1600). Anal.

calcd for $C_{56}H_{40}ClN_7O_4RuS \cdot 3H_2O$: C, 55.06; H, 3.80; N, 10.32. Found: C, 55.35; H, 3.68; N, 9.97%.

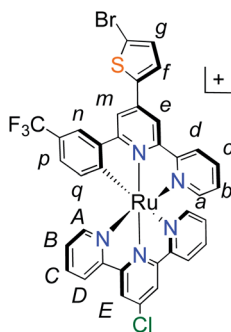
[Ru(CO₂HTPathiotpy)(tpy-OH)][(Cl)₂] (K1). In a 250 mL round-bottom flask, **1b** (77 mg, 0.070 mmol) was dissolved in a THF- H_2O solution (5 : 1, v/v, 30 mL) with KOH (79 mg, 1.3 mmol) and refluxed for overnight. The progress of the reaction was monitored by TLC. After the reaction was complete, the solvent was removed *in vacuo*. The residue was dissolved in 5 mL H_2O and acidified with 0.1 M HCl. The precipitate was collected by filtration and washed with H_2O and Et_2O to yield 52 mg (60%) of the product as a red solid. 1H NMR (400 MHz, MeOD + 1 drop NaOD): δ = 9.12 (s, 2H, H_E), 8.82 (d, 2H, 3J = 8.1 Hz, H_D), 8.37 (d, 2H, 3J = 8.0 Hz, H_d), 8.23 (d, 1H, 3J = 3.9 Hz, H_f), 7.99 (dt, 2H, 3J = 7.9, 4J = 1.4 Hz, H_C), 7.92 (d, 4H, 3J = 8.7 Hz, H_k), 7.85 (dt, 2H, 3J = 7.9 Hz, 4J = 1.4 Hz, H_c), 7.81 (s, 1H, H_e), 7.78 (d, 2H, 3J = 8.7 Hz, H_h), 7.67 (d, 2H, 3J = 4.9 Hz, H_A), 7.61 (d, 1H, 3J = 3.9 Hz, H_g), 7.37–7.32 (m, 4H, H_B , H_b), 7.19 (d, 2H, 3J = 8.7 Hz, H_i), 7.11–7.06 (m, 6H, H_j , H_a); HRMS (MALDI-TOF): m/z = 996.1511 [$(M)^+$] (calcd for $C_{54}H_{36}N_7O_5RuS^+$: m/z = 996.1551). Anal. calcd for $C_{41}H_{30}Cl_3N_4O_4RuS \cdot 2H_2O$: C, 58.75; H, 3.74; N, 8.88. Found: C, 59.12; H, 3.85; N, 8.97%.



4,4'-(4-(4,4,5,5-Tetramethyl-1,3,2-dioxaborolan-2-yl)phenylazanediyl)dibenzoate (P2b). A Schlenk flask under N_2 was loaded with $Pd(dppf)Cl_2$ (35 mg, 0.050 mmol), KOAc (0.286 g, 2.91 mmol) and bis(pinacolato)diboron (0.259 g, 1.02 mmol). DMSO (10 mL, stored over molecular sieves and degassed with N_2) and 4,4'-(4-(4,4,5,5-tetramethyl-1,3,2-dioxaborolan-2-yl)phenylazanediyl)dibenzoic acid^{23,24} (0.400 g, 0.970 mmol) were added to the flask. The mixture was stirred at 80 °C for 24 h under N_2 . CH_2Cl_2 (50 mL) was added to the flask. The mixture was washed with water (3 × 50 mL) to remove the DMSO. The organic layer was dried over $MgSO_4$, filtered and the solvent removed *in vacuo*. The residue was purified by column chromatography [SiO_2 : CH_2Cl_2 - CH_3OH (9 : 1), R_f = 0.46] to yield 0.19 g (43%) of the product as a white solid. The product was used immediately used without further purification. 1H NMR (400 MHz, $CDCl_3$): δ = 7.93 (d, 4H, 3J = 8.8 Hz, H_k), 7.76 (d, 2H, 3J = 8.5 Hz, H_h), 7.11–7.08 (m, 6H, H_j , H_i), 1.22 (s, 12H, H_r); HRMS (MALDI-TOF): m/z = 459.1848 [$(M)^+$] (calcd for $C_{26}H_{26}BNO_6^+$: m/z = 458.1884).

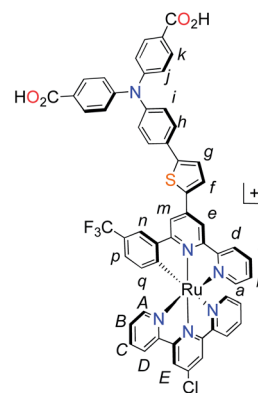


[Ru(P2a)(L2)][NO₃] (2b). In a 250 mL RBF, Ru(L2)Cl₃ (0.100 g, 0.210 mmol) and the **P2a** (97 mg, 0.21 mmol) were dissolved in an MeOH–H₂O solution (5 : 1, v/v, 52 mL) with *n*-ethylmorpholine (5 drops). The solution was left to reflux for 16 h. AgNO₃ (36 mg, 21 mmol) was added and the solution refluxed for an additional 2 h. The solvent was removed *in vacuo* and the residue purified by column chromatography [SiO₂: CH₂Cl₂–MeOH, (9 : 1, v/v), *R_f* = 0.31] to yield 0.111 g (59%) as a black powder. ¹H NMR (400 MHz, CD₃OD): δ = 8.90 (s, 2H, *H_E*), 8.77–8.76 (m, 2H, *H_d*, *H_m*), 8.60–8.59 (m, 3H, *H_D*, *H_e*), 8.22 (s, 1H, *H_n*), 7.97–7.93 (m, 2H, *H_f*, *H_c*), 7.87 (dd, 2H, ³*J* = 8.2 Hz, ³*J* = 8.2 Hz, ³*J* = 8.1 Hz, *H_C*), 7.55 (d, 1H, ³*J* = 4.7 Hz, *H_a*), 7.49 (d, 2H, ³*J* = 5.2 Hz, *H_A*), 7.38 (d, 1H, ³*J* = 4.0 Hz, *H_g*), 7.19–7.13 (m, 3H, *H_B*, *H_b*), 6.76 (d, 1H, ³*J* = 7.9 Hz, *H_p*), 5.95 (d, 1H, ³*J* = 7.8 Hz, *H_q*). HRMS (ESI): *m/z* = 829.9353 [(M)⁺] (calcd for C₃₆H₂₁BrClF₃N₅O₂RuS⁺: *m/z* = 829.9372). Anal. calcd for C₃₆H₂₁BrClF₃N₅O₃RuS·2H₂O: C, 46.64; H, 2.72; N, 9.06. Found: C, 46.83; H, 2.47; N, 9.18%.



[Ru(CO₂HTPAthioCF₃pbpy)(tpy-Cl)][PF₆] (K2). In a 100 mL Schlenk flask under an N₂ atmosphere, **2b** (0.111 g, 0.125 mmol), **P2b** (0.060 g, 0.131 mmol), K₂CO₃ (0.172 g, 1.24 mmol) and the Pd(PPh₃)₄ (0.015 g, 0.013 mmol) was added with 30 mL anhydrous DMF. The reaction was stirred at 70 °C for 14 h. After cooling to room temperature the solution was filtered and subsequently washed with DMF and water. The purple filtrate was acidified with 0.1 M HPF₆ and the solid was collected by filtration. The solid was purified by column chromatography [SiO₂: 8 : 2 acetone–MeOH, *R_f* = 0.15] to yield 0.045 g (29.5%) of the product as a dark black solid. ¹H NMR (400 MHz, MeOD): δ = 8.90 (s, 2H, *H_E*), 8.83 (s, 1H, *H_e*), 8.78 (d, 1H, ³*J* = 7.6 Hz, *H_a*), 8.67 (s, 1H, *H_d*), 8.60 (d, 2H, ³*J* = 7.6 Hz, *H_D*), 8.22 (s, 1H, *H_m*), 8.15 (d, 1H, ³*J* = 3.9 Hz, *H_f*), 7.97–7.90 (m, 5H, *H_C*, *H_k*), 7.82 (t, 2H, ³*J* = 7.9 Hz, *H_B*), 7.75 (d, 2H, ³*J* = 8.6 Hz, *H_h*), 7.58 (d, 1H, ³*J* = 3.9 Hz, *H_g*), 7.54–7.53 (m, 3H, *H_n*, *H_A*), 7.18–7.15 (m, 5H, *H_i*, *H_b*, *H_C*), 7.08 (d, 4H, ³*J* = 8.7 Hz, *H_j*), 6.75 (d, 1H, ³*J* = 7.9 Hz, *H_p*), 5.93 (d, 1H, ³*J* = 8.0 Hz, *H_q*). HRMS (ESI):

m/z = 1081.11283 [(M)⁺] (calcd for C₅₆H₃₅ClF₃N₆O₄RuS⁺: *m/z* = 1081.11304). Anal. calcd for C₅₆H₃₅ClF₃N₆O₄PRuS·H₂O: C, 54.05; H, 3.00; N, 6.75. Found: C, 54.28; H, 2.94; N, 6.60%.



Physical methods

Elemental analysis (EA), electrospray ionization (ESI) and matrix assisted laser desorption ionization time of flight (MALDI-TOF) mass spectrometry (MS) data were collected at the Chemistry Instrumentation Facility of the University of Calgary. Electrochemical measurements were performed under anaerobic conditions with a Princeton Applied Research VersaStat 3 potentiostat using dry solvents, Pt working and counter electrodes, Ag pseudoreference electrode, and 0.1 M NBu₄BF₄ DMF solutions. Electronic spectroscopic data were collected on CH₃OH solutions using a Cary 5000 UV-visible spectrophotometer (Varian).

Samples for infrared absorption spectroscopy were prepared as either a KBr pressed disk (dye only), by adsorbing the dye on a mesoporous NiO film deposited on a CaF₂ window (Crystran). The NiO films were prepared by spraying a saturated solution of NiCl₂ in acetylacetone onto the surface of the CaF₂ window which was pre-heated to 450 °C on a hotplate; this was then allowed to cool slowly to room temperature to give a compact film of NiO. The mesoporous layer was then deposited on top of the compact layer using an F108-templated precursor solution containing NiCl₂ (1 g), Pluronic® co-polymer F108 (1 g), Milli-Q water (3 g) and ethanol (6 g) and a doctor blade was used to remove the excess. The film was sintered at 450 °C for 30 minutes and an additional layer of precursor solution was applied and sintered to increase the film thickness. Infrared spectra were recorded on a Thermo Nicolet 380 FTIR spectrometer for 16 scans at a resolution of 2 cm⁻¹.

NiO electrodes were made by applying the precursor solution described in previous literature by doctor blade onto conducting glass substrates (Pilkington TEC15, sheet resistance 15 Ω per square) using Scotch tape as a spacer (0.2 cm² active area), followed by sintering in a Nabertherm B150 oven at 450 °C for 30 min. The NiO electrodes were soaked in a dichloromethane solution of the dye (0.3 mM) for 16 h at room temperature.³⁰ The dyed NiO electrode was assembled face-to-face with a platinized counter electrode (Pilkington TEC8, sheet resistance 8 Ω per square) using a 30 μm thick thermoplastic frame (Surlyn 1702).

The electrolyte, containing LiI (1.0 M) and I₂ (0.1 M) in acetonitrile, was introduced through the pre-drilled hole in the counter electrode, which was sealed afterwards. The cells were measured 12 hours after assembly. The UV-visible absorption spectra of the dyes adsorbed on NiO films were recorded using an Ocean Optics USB2000+VIS-NIR fibre-optic spectrophotometer. Incident photon-to-current conversion efficiencies were recorded using monochromatic light from a system consisting of a Xenon lamp, a monochromator and appropriate filters and calibrated against a certified reference Si photodiode. Current-voltage measurements were measured using an Ivium CompactStat potentiostat under simulated sunlight from an Oriel 150 W solar simulator, giving light with an intensity of 100 mW cm⁻².

Computational details

Geometries of both were optimised in the gas phase by DFT using the B3LYP hybrid functional (20% Hartree-Fock)³¹ as implemented in the NWChem 6.1 software package.³² Stuttgart-Dresden relativistic small core potential basis set was used for Ru (ref. 33) and 6-311G* basis sets were used for all other atoms.³⁴ Single-point calculations using the same basis sets and functional were carried out using the COSMO solvation model³⁵ for methanol ($\epsilon = 32.7$, $R_{\text{solv}} = 1.3 \text{ \AA}$). The energies and plots of HOMO-10 up to LUMO+10 were calculated. Molecular orbital plots were visualised with the ECCE (Pacific Northwest National Laboratory) software package.³⁶ Time-dependent DFT (TD-DFT) calculations were carried out using the same B3LYP functional, basis sets and COSMO solvation model for methanol on the optimised geometries to calculate electronic absorption spectra. The 50 lowest energy spin-allowed transitions were calculated for each dye. No triplet excited state transitions were calculated.

Results

Dye synthesis

The methyl ester TPA precursor (**P1a**) was synthesized by a modification of a literature procedure^{23,24} and subsequently converted to the boronic ester (**P1b**) using a palladium-catalyzed Miyaura reaction of **P1a** with bis(pinacolato)diboron (Fig. 2).³⁷ Under Suzuki cross-coupling conditions **P1b** was reacted with **P1c** to yield **L1** in moderate yields.

With the ligand **L1** in hand, the synthesis of **K1** was straightforward using established synthetic routes involving the subsequent coordination of **L1** and **L2** to the ruthenium metal center (Fig. 3).^{28,38,39} An unexpected reaction occurred upon saponification of the methyl ester units to carboxylic acids: chloride substitution by the hydroxide species in solution was observed, most likely occurring *via* a nucleophilic aromatic substitution reaction.

Unlike the polypyridyl p-type sensitizer (**K1**), the synthesis of the cyclometalated sensitizer **K2** was achieved following a modification of the synthesis previously reported (Fig. 4).⁴⁰ Cycloruthenation of the precursor Ru(**L2**)Cl₃ with **P2a** yielded the intermediary compound **2b** in moderated yields. The TPA moiety was installed *via* cross-coupling conditions using **P2b** to yield **2** after acidic workup.

Optical and electrochemical characterization

The UV-visible absorption spectra of the dyes, **K1** and **K2** in methanol solution and adsorbed on NiO films are shown in Fig. 5. The electronic distributions in the frontier orbitals were calculated for **K1** and **K2** in methanol using DFT and the TDDFT results were compared to the electronic spectra (Fig. 6 and 7). In both complexes the electronic distribution of the HOMO is predicted to be localized over the triphenylamine and thiophene donor. The predominant compositions to the principle electronic transitions with their wavelengths and calculated oscillator strengths (*f*) are provided in Tables S4 and S5.† Both dyes exhibit one prominent band, appearing at 523 ± 1 nm ($\epsilon = 4.73$ and $3.34 \times 10^4 \text{ L mol}^{-1} \text{ cm}^{-1}$ for **K1** and **K2** respectively). Results from TD-DFT calculations suggest that this transition may be assigned to a favourable intraligand charge-transfer (ILCT) transition arising principally from the triphenylamine- and thiophene-based HOMO to the terpyridyl-based LUMO in **K1** or 3-(trifluoromethyl)phenyl-2,2'-bipyridine-based LUMO in **K2**.

In addition to the band at 523 nm the spectrum for **K1** contains a shoulder at *ca.* 470 nm, which we have assigned to the MLCT transition involving the HOMO-3 and the due to the lower intensity and higher energy required for excitation. This would be more in agreement with 4'-chloro-2,2':6',2''-terpyridine ruthenium(II) ($\lambda_{\text{max}} = 480 \text{ nm}$, $\epsilon = 16\,000 \text{ L mol}^{-1} \text{ cm}^{-1}$)

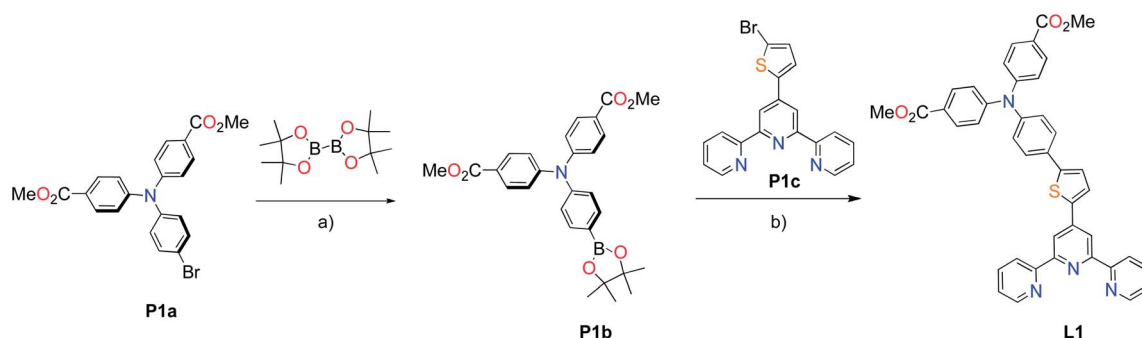


Fig. 2 Synthesis of **L1**. Reaction conditions: (a) Pd(dppf)Cl₂, KOAc, DMSO, 80 °C, 6 h, N₂; (b) Pd(PPh₃)₄, K₂CO₃, THF-H₂O (9 : 1, v/v), reflux, 20 h, N₂.

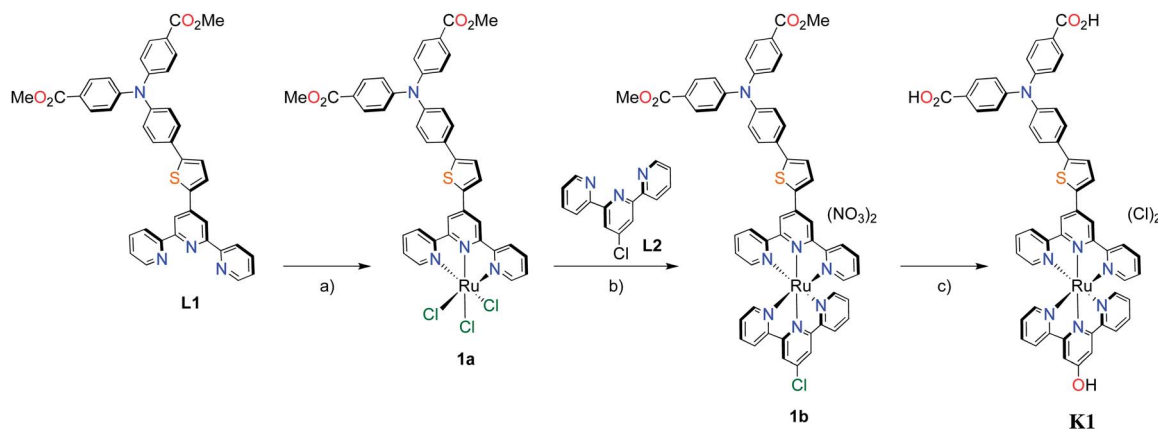


Fig. 3 Synthesis of polypyridyl p-type sensitizer (**K1**). Reaction conditions: (a) $\text{RuCl}_3 \cdot 3\text{H}_2\text{O}$, abs. EtOH, reflux, 4 h; (b) (i) EtOH, *n*-ethylmorpholine, reflux, 20 h. (ii) AgNO_3 , reflux, 2 h; (c) KOH, THF– H_2O (5 : 1, v/v).

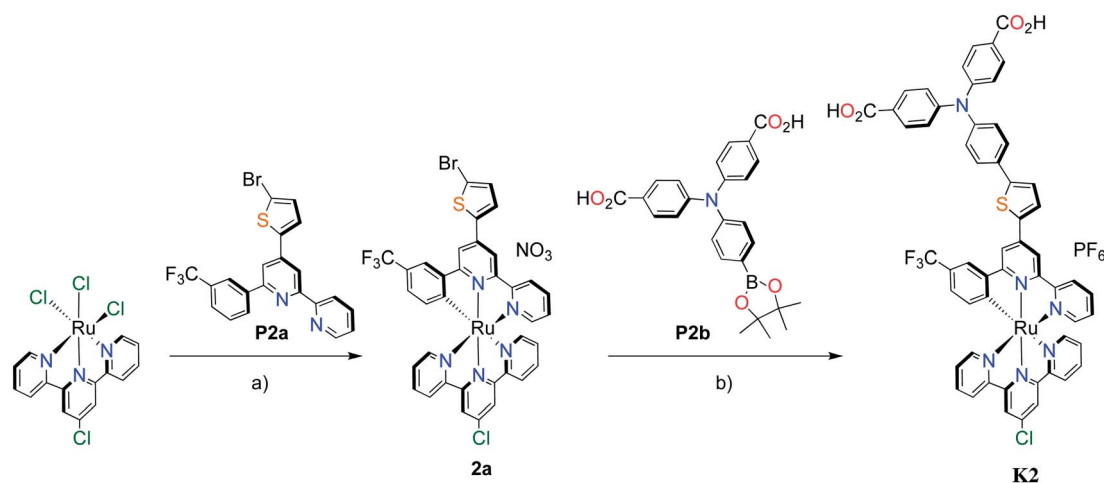


Fig. 4 Synthesis of cyclometalated p-type sensitizer (**K2**). Reaction conditions: (a) MeOH– H_2O (5 : 1, v/v), *n*-ethylmorpholine, reflux, 16 h; (b) $\text{Pd}(\text{PPh}_3)_4$, K_2CO_3 , DMF, 70 °C, 14 h, N_2 .

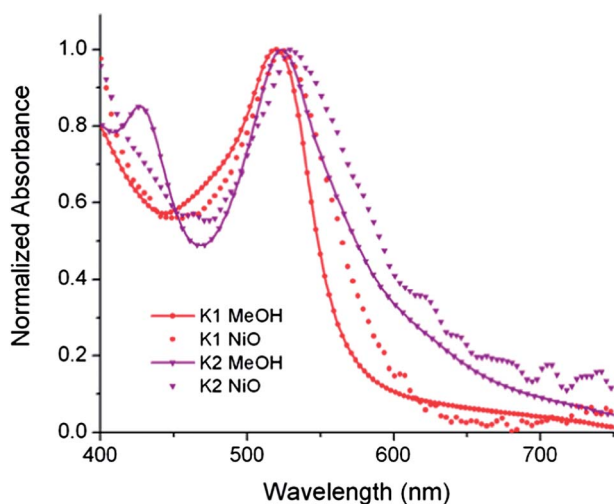


Fig. 5 The absorption spectra of **K1** (red) and **K2** (purple) in MeOH solution (A) and adsorbed onto NiO films on CaF windows (B).

and 4'-hydroxy-2,2':6',2'-terpyridine ruthenium(II) ($\lambda_{\text{max}} = 485 \text{ nm}$, $\epsilon = 12\,700 \text{ L mol}^{-1} \text{ cm}^{-1}$).⁴¹

The absorption spectrum of **K2** in solution is even more broadened compared to **K1** suggesting a number of overlapping ILCT and MLCT transitions contribute to the spectrum. The large extinction coefficient of the predominant lower energy band for **K2** in solution is similar to the intraligand transition at 505 nm ($\epsilon = 42\,000$) for the analogous complex “3” in ref. 38 in which the electron withdrawing $-\text{CO}_2\text{H}$ groups are absent. In the reported complex a MLCT transition was assigned to a shoulder at 440 nm ($\epsilon = 19\,400 \text{ L mol}^{-1} \text{ cm}^{-1}$). According to our TD-DFT calculations, the lowest energy transition is due to the promotion of an electron from HOMO–2, where the electron density is distributed over the anionic portion of the ligand and the ruthenium centre, to the LUMO+1 where the electron density is predominantly localized on the terpyridine acceptor ligand. The predominant band at 524 nm is a combination of the intraligand charge transfer HOMO \rightarrow LUMO and the promotion of the electron from the HOMO to the π^* orbitals on

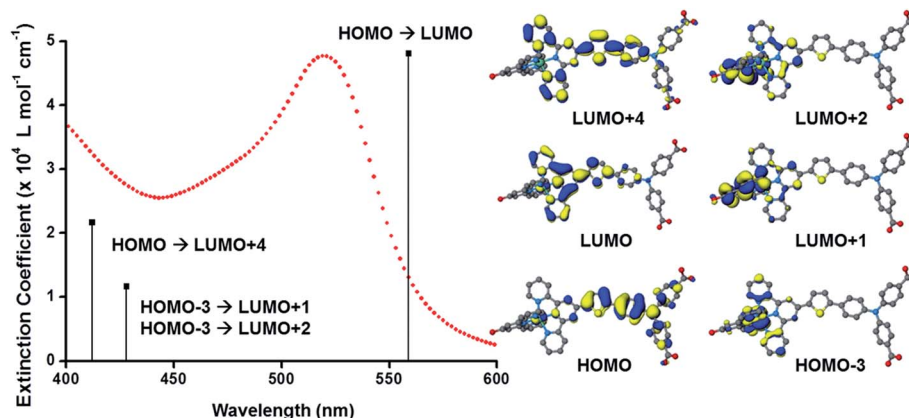


Fig. 6 (Left) Plot of the ground state electronic absorption spectrum of **K1** in methanol with calculated electronic transitions and their relative intensities; (right) optimised geometries and frontier orbitals of **K1** in methanol performed using the B3LYP hybrid functional (20% Hartree–Fock) using the COSMO solvation model.

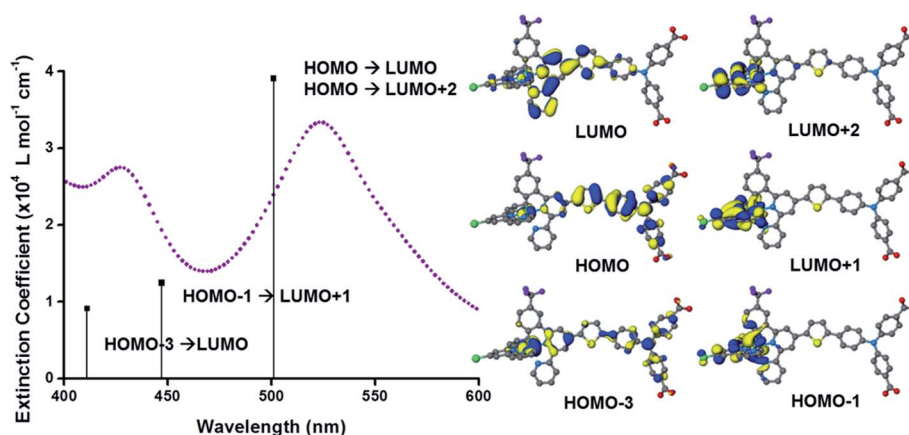


Fig. 7 (Left) Plot of the ground state electronic absorption spectrum of **K2** in methanol with calculated electronic transitions and their relative intensities; (right) optimised geometries and frontier orbitals of **K2** in methanol performed using the B3LYP hybrid functional (20% Hartree–Fock) using the COSMO solvation model.

the terpyridine (LUMO+2). The higher energy band is likely to be due to another intraligand charge transfer (HOMO \rightarrow LUMO+3). Therefore the predominant electronic transitions contributing to the visible absorption spectrum involve a transfer of electron density away from the donor ligand and therefore the NiO surface when adsorbed through the carboxylate groups which is favorable for sensitization of NiO. The FTIR spectra for the anchored dyes is given in Fig. S3.† Adsorption on NiO did not markedly affect the visible absorption spectrum of the dyes indicating that the electronic structure of the chromophore is unaffected by binding.

Table 1 summarises the optical and electrochemical characterisation data for **K1** and **K2**. The redox potential of **L1** here is 1.34 V vs. NHE, 100 mV more positive than the “L3” ligand in ref. 38 in which the electron withdrawing $-\text{CO}_2\text{H}$ groups are absent. The corresponding bis-terpyridyl ruthenium complex had a similar redox potential and so for complex **K1** we are confident that the first oxidation at 1.38 V vs. NHE is triphenylamine centred as in agreement with the DFT calculations. We were

unable to resolve the Ru(III/II) couple for **K1** but we expect it to lie between the redox potential of bis-4'-hydroxy-2,2':6',2'-terpyridyl ruthenium (1.36 V vs. NHE) and bis-4'-(*p*-tolyl)-2,2':6',2'-terpyridyl ruthenium (1.5 V vs. NHE).⁴¹ For **K2** we observed again an oxidation process likely to be oxidation of triphenylamine at 1.40 V vs. NHE in agreement with the DFT calculations which place the HOMO in **K2** only 3 eV lower in energy than the HOMO in **K1**. The first oxidation process, however, was found to be at 0.93 V vs. NHE which is closer to that of the cyclometalated complexes reported by Ji *et al.* and so we have assigned this to the Ru(III/II) couple.²⁰ The appearance of the Ru(III/II) couple was observed for the analogous complex “4” in ref. 39 which differed from **K2** by the substituents on the triphenylamine (electron donating $-\text{OMe}$ rather than electron withdrawing $-\text{CO}_2\text{H}$) and an electron withdrawing trimethyl-4,4',4''-tricarboxylate-2,2':6',2'-terpyridine ligand. For the previously reported complex the oxidation of the triphenylamine moiety at 1.19 V vs. NHE was accompanied by a reversible Ru(III/II) couple at 1.27 V vs. NHE. Therefore, analogous to similar dyes used for n-type DSCs and in

Table 1 Optical and electrochemical properties of the dyes K1 and K2

Dye	Absorption			E_{0-0}^c (eV)	E^{nd} (V vs. NHE)		$E_{D/D-}^e$ (V vs. NHE)
	λ_{max}^a (nm)	ϵ at λ_{max}^a ($\times 10^4$ L mol $^{-1}$ cm $^{-1}$)	λ_{max} on NiO b (nm)		TPA $^{+/0}$	Ru $^{III/II}$	
K1	523	4.73	525	2.1	1.38	ca. 1.5	-0.73
K2	524	3.34	531	1.9	1.40	0.93	-0.50

^a Absorption spectra were measured in MeOH at room temperature. ^b Absorption spectra of sensitized NiO films. ^c E_{0-0} was estimated from 10% onset point of absorption spectra in MeOH. ^d The redox potential of the dyes were measured in DMF with 0.1 M tetrabutylammonium tetrafluoroborate (TBABF $_4$) as a supporting electrolyte (working electrode: glassy carbon; reference electrode: Ag/Ag $^+$ calibrated with ferrocene/ferrocenium (Fc $^{+/0}$) as an internal reference and converted to NHE by addition of 690 mV, counter electrode: Pt). ^e First reduction potential of the dyes were estimated from $E(\text{TPA}^{+/0})$ plus E_{0-0} .

agreement with our DFT studies we have increased the electron density of the dye at the ruthenium centre for **K2** compared to the **K1**. The dramatic shift in the first electrode potential demonstrates that the negatively charged σ -donor ligand stabilises the Ru(III) and therefore ought to stabilise the MLCT compared to the terpyridyl ligand.

The dyes were found to be only weakly emissive and so the E_{0-0} energies were estimated from the onset of the wavelength at which the absorption was 10% of the maximum. The values for the electrode potential for the TPA $^{+/0}$ couple is much more positive than the valence band of NiO so there should be a sufficient driving force for hole injection from the dye to the semiconductor. The reduction potential of these dyes adsorbed on NiO are in the range of -0.5 V to -0.75 V vs. NHE which suggests that regeneration of the dyes by I_3^-/I^- is strongly favourable.⁴²

p-Type dye-sensitized solar cells

The photovoltaic performance of solar cells based on these dyes is summarized in Table 2. Sandwich-type solar cells were assembled using **K1** and **K2** sensitized nanocrystalline NiO as the working electrodes, platinized conducting glass as the counter electrode and 1.0 M LiI, 0.1 M I $_2$ in acetonitrile as the electrolyte. DSCs based on **K1** produced a maximum incident photon to current conversion efficiency (IPCE) of 14%, whereas under the same conditions, the devices based on **K2** gave a similar maximum IPCE of 9%. This followed the trend in photocurrent measured using simulated sunlight shown in Fig. 8. DSCs using **K1** and **K2** utilising a cobalt based redox couple (0.1 M Co(dtb) $_3$ (ClO $_4$) $_3$ (2)) gave a negligible photocurrent (see Fig. S9 †). This suggests that, despite our efforts the rate of charge recombination between the reduced dye and the holes in

Table 2 Photovoltaic performance of DSCs based on K1 and K2^a

Dye	J_{SC} (mA cm $^{-2}$)	V_{OC} (mV)	FF	η (%)	IPCE $_{max}$ (%)
K1	2.91	96	0.32	0.09	14
K2	1.96	93	0.39	0.07	9

^a J_{SC} is the short-circuit current density at the $V = 0$ intercept; V_{OC} is the open-circuit voltage at the $J = 0$ intercept; FF is the device fill factor; η is the power conversion efficiency; IPCE $_{max}$ is the maximum monochromatic incident photon-to-current conversion efficiency.

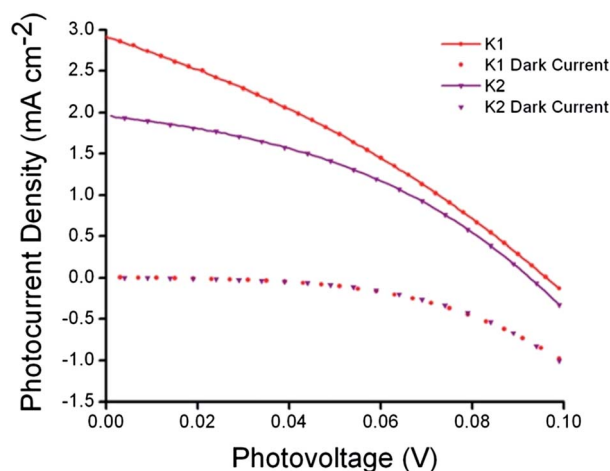


Fig. 8 Current–voltage characteristics (right) of K1 (red) and K2 (purple) sensitized NiO solar cells under AM 1.5G (100 mW cm $^{-2}$) illumination.

the NiO may still be too fast for the charge on the dye to be intercepted by the cobalt(III) ($\tau = 1\text{--}10$ μ s).^{8,43} Nonetheless the results with I_3^-/I^- were significantly better than that typically obtained from ruthenium dyes reported elsewhere^{14,17,19} (<1 mA cm $^{-2}$) and the current obtained for **K2** was comparable to the cyclometalated ruthenium dye reported by Ji *et al.*²⁰

Conclusions

We have developed and tested a series of new ruthenium-based sensitizers for NiO based p-DSCs. This work demonstrates that our dye-design is superior to applying “classic” Ru(bpy) $_3^{2+}$ derivatives used for TiO $_2$ -sensitization in p-DSCs. The complex ligand system dominates the optoelectronic properties of the dye, greatly increasing the extinction coefficients. Whilst the high extinction coefficients are necessary for efficient light collection from NiO photocathodes the efficiency is still limited by recombination reactions preventing the use of alternative cobalt-based redox shuttles. We envisage that better use of triplet states of heavy transition metals could lead to longer lived charge separation that is required for p-DSCs to be as efficient as their TiO $_2$ equivalents, leading to efficient tandem devices that have a theoretical maximum efficiency that

surpasses those of their single photo-electrode components and further work towards achieving this goal is ongoing.

Acknowledgements

EAG thanks the Royal Society for a Dorothy Hodgkin Research Fellowship. As a member of the UK HPC Materials Chemistry Consortium PIPE acknowledges the EPSRC (grant no. EP/F067496) and the UK's national supercomputing service HECToR as well as the Huddersfield Centre for High Performance Computing for computational resources utilised in this work. The Canadian authors thank National Science & Engineering Research Council (Canada), Canadian Research Chairs and the Alfred P. Sloan Foundation for support.

References

- 1 A. Hagfeldt, G. Boschloo, L. Sun, L. Kloo and H. Pettersson, *Chem. Rev.*, 2010, 6595–6663.
- 2 A. Hagfeldt, U. B. Cappel, G. Boschloo, L. Sun, L. Kloo, H. Pettersson and E. A. Gibson, Dye-Sensitized Photoelectrochemical Cells, in *Practical Handbook of Photovoltaics Fundamentals and Applications*, ed. A. McEvoy, T. Markvart and L. Castaner, Academic Press/Elsevier Ltd., Oxford, 2012, pp. 479–542.
- 3 M. Wang, P. Chen, R. Humphry-Baker, S. M. Zakeeruddin and M. Grätzel, *ChemPhysChem*, 2009, 10, 290–299.
- 4 L. Vallejo, A. William, S. Quiñones, A. Cesar and S. J. A. Hernandez, The Chemistry and Physics of Dye-Sensitized Solar Cells, in *Solar Cells – Dye-Sensitized Devices*, ed. L. A. Kosyachenko, Tech Europe, 2011, pp. 399–418.
- 5 S. Wenger, S. Seyrling, A. N. Tiwari and M. Grätzel, *Appl. Phys. Lett.*, 2009, 94, 173508.
- 6 J. He, H. Lindström, A. Hagfeldt and S. Lindquist, *Sol. Energy Mater. Sol. Cells*, 2000, 62, 265–273.
- 7 A. Nattestad, A. J. Mozer, M. K. R. Fischer, Y.-B. Cheng, A. Mishra, P. Bäuerle and U. Bach, *Nat. Mater.*, 2010, 9, 31–35.
- 8 E. A. Gibson, A. L. Smeigh, L. Le Pleux, J. Fortage, G. Boschloo, E. Blart, Y. Pellegrin, F. Odobel, A. Hagfeldt and L. Hammarström, *Angew. Chem., Int. Ed. Engl.*, 2009, 48, 4402–4405.
- 9 F. Odobel, Y. Pellegrin, E. A. Gibson, A. Hagfeldt, A. L. Smeigh and L. Hammarström, *Coord. Chem. Rev.*, 2012, 256, 2414–2423.
- 10 P. Qin, J. Wiberg, E. A. Gibson, M. Linder, L. Li, T. Brinck, A. Hagfeldt, B. Albinsson and L. Sun, *J. Phys. Chem. C*, 2010, 114, 4738–4748.
- 11 A. Morandeira, G. Boschloo, A. Hagfeldt and L. Hammarström, *J. Phys. Chem. B*, 2005, 109, 19403–19410.
- 12 A. L. Smeigh, L. Le Pleux, J. Fortage, Y. Pellegrin, E. Blart, F. Odobel and L. Hammarström, *Chem. Commun.*, 2012, 48, 678–680.
- 13 M. Borgström, E. Blart, G. Boschloo, E. Mukhtar, A. Hagfeldt, L. Hammarström and F. Odobel, *J. Phys. Chem. B*, 2005, 109, 22928–22934.
- 14 A. Nattestad, M. Ferguson, R. Kerr, Y.-B. Cheng and U. Bach, *Nanotechnology*, 2008, 19, 295304.
- 15 P. Qin, H. Zhu, T. Edvinsson, G. Boschloo, A. Hagfeldt and L. Sun, *J. Am. Chem. Soc.*, 2008, 130, 8570–8571.
- 16 Y.-S. Yen, W.-T. Chen, C.-Y. Hsu, H.-H. Chou, J. T. Lin and M.-C. P. Yeh, *Org. Lett.*, 2011, 13, 4930–4933.
- 17 Y. Pellegrin, L. Le Pleux, E. Blart, A. Renaud, B. Chavillon, N. Szuwarski, M. Boujtita, L. Cario, S. Jobic, D. Jacquemin, *et al.*, *J. Photochem. Photobiol., A*, 2011, 219, 235–242.
- 18 M. Bräutigam, M. Schulz, J. Inglis, J. Popp, J. G. Vos and B. Dietzek, *Phys. Chem. Chem. Phys.*, 2012, 14, 15185–15190.
- 19 J. C. Freys, J. M. Gardner, L. D'Amario, A. M. Brown and L. Hammarström, *Dalton Trans.*, 2012, 41, 13105–13111.
- 20 Z. Ji, G. Natu, Z. Huang, O. Kokhan, X. Zhang and Y. Wu, *J. Phys. Chem. C*, 2012, 116, 16854–16863.
- 21 K. C. D. Robson, P. G. Bomben and C. P. Berlinguette, *Dalton Trans.*, 2012, 41, 7814–7829.
- 22 P. G. Bomben, T. J. Gordon, E. Schott and C. P. Berlinguette, *Angew. Chem., Int. Ed. Engl.*, 2011, 50, 10682–10685.
- 23 K. Ghosh, G. Masanta and A. P. Chattopadhyay, *Eur. J. Org. Chem.*, 2009, 4515–4524.
- 24 K. Ghosh, G. Masanta, R. Fröhlich, I. D. Petsalakis and G. Theodorakopoulos, *J. Phys. Chem. B*, 2009, 113, 7800–7809.
- 25 M. Beley, D. Delabouglise, G. Houppy, J. Husson and J.-P. Petit, *Inorg. Chim. Acta*, 2005, 358, 3075–3083.
- 26 R. López, D. Villagra, G. Ferraudi, S. A. Moya and J. Guerrero, *Inorg. Chim. Acta*, 2004, 357, 3525–3531.
- 27 E. C. Constable and M. D. Ward, *J. Chem. Soc., Dalton Trans.*, 1990, 1405.
- 28 K. C. D. Robson, B. D. Koivisto, A. Yella, B. Spornova, M. K. Nazeeruddin, T. Baumgartner, M. Grätzel and C. P. Berlinguette, *Inorg. Chem.*, 2011, 50, 5494–5508.
- 29 D. J. Wasylenko, C. Ganesamoorthy, B. D. Koivisto, M. A. Henderson and C. P. Berlinguette, *Inorg. Chem.*, 2010, 49, 2202–2209.
- 30 S. Sumikura, S. Mori, S. Shimizu, H. Usami and E. Suzuki, *J. Photochem. Photobiol., A*, 2008, 199, 1–7.
- 31 P. J. Stephens, F. J. Devlin, C. F. Chabalowski and M. J. Frisch, *J. Phys. Chem.*, 1994, 98, 11623–11627.
- 32 M. Valiev, E. J. Bylaska, N. Govind, K. Kowalski, T. P. Straatsma, H. J. J. van Dam, D. Wang, J. Nieplocha, E. Apra, T. L. Windus, *et al.*, *Comput. Phys. Commun.*, 2010, 181, 1477.
- 33 D. Andrae, U. Haussermann, M. Dolg, H. Stoll and H. Preuss, *Theor. Chim. Acta*, 1990, 77, 123–141.
- 34 R. Krishnan, J. S. Binkley, R. Seegar and J. A. Pople, *J. Chem. Phys.*, 1980, 72, 650–654.
- 35 A. Klamt and G. Schüürmann, *J. Chem. Soc., Perkin Trans. 2*, 1993, 799.
- 36 G. Black, K. Schuchardt, D. Gracio, B. Palmer and K. Schuchardt, *The Extensible Computational Chemistry Environment: A Problem Solving Environment for High Performance Theoretical Chemistry*, 2003, pp. 122–131.

- 37 C. J. Aspley and J. A. G. Williams, *New J. Chem.*, 2001, **25**, 1136–1147.
- 38 K. C. D. Robson, B. D. Koivisto, T. J. Gordon, T. Baumgartner and C. P. Berlinguette, *Inorg. Chem.*, 2010, **49**, 5335–5337.
- 39 K. C. D. Robson, B. Spornova, B. D. Koivisto, E. Schott, D. G. Brown and C. P. Berlinguette, *Inorg. Chem.*, 2011, **50**, 6019–6028.
- 40 K. C. D. Robson, B. D. Koivisto and C. P. Berlinguette, *Inorg. Chem.*, 2012, **51**, 1501–1507.
- 41 J. Sauvage, J. Collin, J. Chambron, S. Guillerez, C. Coudret, V. Balzani, B. Francesco, L. De Cola and L. Flamigni, *Chem. Rev.*, 1994, **94**, 993–1019.
- 42 E. A. Gibson, L. Le Pleux, J. Fortage, Y. Pellegrin, E. Blart, F. Odobel, A. Hagfeldt and G. Boschloo, *Langmuir*, 2012, **28**, 6485–6493.
- 43 L. Le Pleux, A. L. Smeigh, E. Gibson, Y. Pellegrin, E. Blart, G. Boschloo, A. Hagfeldt, L. Hammarström and F. Odobel, *Energy Environ. Sci.*, 2011, **4**, 2075.